Analysis of the diagnostic value of CT radiomics models in differentiating GIST and other mesenchymal tumors

Bin Du[1] **MD,**
Zhihui Zhu[1] **MD,**
Jin Pu[2] **MD,**
Yaqin Zhao[3] **MD,**
Shichao Wang[1] **MD**

1. Department of Radiotherapy Physics & Technology, West China Hospital, Sichuan University, Chengdu, China
2. Department of Radiology, West China Hospital, Sichuan University, Chengdu, China
3. Department of Abdominal Oncology, West China Hospital, Sichuan University, Chengdu, China

Keywords: CT radiomics model - GIST - Mesenchymal tumor - Leiomyoma - Schwannoma - Machine learning - Differential diagnosis.

Corresponding author:
Shichao Wang MD,
Department of Radiotherapy Physics & Technology, West China Hospital, Sichuan University, Chengdu, China
sospy73877@tom.com

Received:
20 July 2024
Accepted revised:
8 August 2024

Abstract

Objective: To analyze the diagnostic value of computed tomography (CT) radiomics models in differentiating gastrointestinal stromal tumors (GIST) and other mesenchymal tumors. **Materials and Methods:** A retrospective analysis of clinical data from 153 patients with pathologically confirmed gastrointestinal mesenchymal tumors treated in our hospital from July 2019 to March 2024 was conducted, including 107 cases of GIST, 18 cases of leiomyoma, and 28 cases of schwannoma. LASSO regression was used for feature selection. Logistic regression and Random Forest (RF) models were established based on selected features using machine learning algorithms, with the dataset divided into training (107 cases) and validation sets (46 cases) at a 7:3 ratio. The diagnostic performance of the models was evaluated using receiver operating characteristic (ROC) curves. **Results:** In the training set, there were significant differences between GIST and non-GIST in terms of enhancement degree, age, maximum diameter, and tumor location distribution ($P<0.05$). A total of 180 radiomics features were extracted using A.K software. LASSO regression reduced the high-dimensional data to 13 radiomics features. Logistic regression and RF models were established based on these 13 features. The AUC for the Logistic regression model was 0.753 in the training set and 0.582 in the validation set, while the AUC for the RF model was 0.941 in the training set and 0.746 in the validation set. The RF model showed higher diagnostic performance than the Logistic regression model ($P< 0.05$). Decision curve analysis showed that the net benefit of the RF model in differentiating GIST was superior to classifying all patients as either GIST or non-GIST and also superior to the Logistic regression model within a probability threshold range of 20%-90%. **Conclusions:** The machine learning models based on radiomics features have good diagnostic value in predicting the pathological classification of GIST and other mesenchymal tumors, with the RF model showing superior diagnostic value compared to the Logistic regression model.

Hell J Nucl Med 2024; 27(2): 141-148 *Published online: 28 August 2024*

Introduction

Gastrointestinal stromal tumors (GIST) are the most common mesenchymal tumors in the gastrointestinal tract, originating from the interstitial cells of Cajal in the gastrointestinal wall, characterized by their aggressiveness and high metastatic potential [1]. Early diagnosis and precise classification of GIST are crucial for selecting appropriate treatment strategies and improving patient prognosis [2]. Currently, the diagnosis of GIST mainly relies on imaging examinations, pathological tests, and immunohistochemical markers [3]. However, traditional imaging techniques such as computed tomography (CT), magnetic resonance imaging (MRI), and positron emission tomography (PET)/CT, although essential for detecting tumor location, size, and morphology, have limitations in distinguishing GIST from other mesenchymal tumors such as leiomyoma and schwannoma [4]. These tumors may appear similar on imaging but differ significantly in biological behavior, treatment approaches, and prognosis, making accurate differentiation clinically significant.

Radiomics is an emerging technology that extracts a large number of quantitative features from imaging data, revealing tumor heterogeneity and microcharacteristics that traditional imaging techniques cannot detect [5]. The core concept of radiomics is to perform deep mining and analysis of medical images through computer algorithms, extracting various features including shape, texture, and intensity, and then establishing quantitative models for tumor classification, diagnosis, and prognosis assessment [6]. Combined with machine learning algorithms, radiomics can significantly improve the utilization efficiency of imaging data and diagnostic accuracy. In recent years, radiomics has shown broad

application prospects in the study of various tumors [7, 8]. For example, in studies of lung cancer, breast cancer, and gliomas, radiomics models have been proven to provide important diagnostic and prognostic information. By extracting imaging features and combining them with machine learning techniques, researchers can construct efficient classification and prediction models to assist clinical decision-making. However, research on radiomics in GIST and other mesenchymal tumors is relatively sparse. Existing studies mainly focus on the preliminary extraction and analysis of imaging features, lacking systematic feature selection, model construction, and validation processes. Especially in terms of large-scale clinical data validation and evaluation of model generalizability, further exploration is needed. Based on this, our study attempts to use CT radiomics technology combined with machine learning algorithms to establish an efficient model capable of differentiating GIST and other mesenchymal tumors and to validate the application value of radiomics in the differential diagnosis of GIST and other mesenchymal tumors. If proven effective, it could provide a new auxiliary tool for clinical diagnosis, helping to improve diagnostic accuracy, optimize treatment plans, and ultimately improve patient clinical outcomes.

Materials and Methods

Basic information

A retrospective analysis was conducted on the clinical data of 153 patients with pathologically confirmed gastrointestinal mesenchymal tumors treated in our hospital from July 2019 to March 2024, including 107 cases of GIST, 18 cases of leiomyoma, and 28 cases of schwannoma. Inclusion criteria: 1) patients had complete preoperative CT enhanced venous phase images; 2) patients were pathologically and immunohistochemically confirmed to have gastrointestinal mesenchymal tumors [9]; 3) tumor diameter >1.5cm; 4) patients aged ≥18 years with complete data available for analysis. Exclusion criteria: 1) patients received relevant treatment before surgery; 2) patients with other tumor diseases or severe internal or external diseases; 3) patients with a history of abdominal surgery; 4) patients with cognitive impairment and/or mental illness. This study was approved by the Medical Ethics Committee.

Examination methods

A 64-slice Philips spiral CT scanner (Netherlands) was used, with patients in a supine position. Scanning parameters: tube voltage 120kV, tube current 380mA, window width 350 HU, window level 10HU, slice thickness 2.5mm, pitch 1.003, rotation time 0.5s, collimation 64×0.625mm, matrix 512×512. Enhanced scanning used non-ionic contrast agent iohexol (0.35mg/mL), injected intravenously using a high-pressure injector at a rate of 3mL/s, with a total contrast volume of 70-90mL. Arterial phase scanning was performed when the CT value of the abdominal aorta reached 100HU, followed by venous phase scanning with a 35s delay.

Image segmentation and feature extraction

Radiomics segmentation and feature calculation

The enhanced abdominal CT venous phase images (DICOM format) were imported into A.K software. One experienced radiologist manually outlined the largest slice of the lesion and the two slices above and below it, avoiding necrotic and cystic areas. The outlined regions of interest (ROI) were fused to obtain a three-dimensional ROI. A.K software was used to calculate 180 radiomics parameters within the ROI, primarily including five categories: Histogram features, Gray Level Size Zone Matrix (GLSZM), Haralick features, Formfactor, and Gray Level Co-occurrence Matrix (GLCM).

Radiomics feature selection

First, the 180 radiomics parameters of the five categories were standardized. Spearman's method in A.K software was used to calculate the redundancy between parameters, with 0.7 set as the redundancy threshold. The retained parameters were dimensionally reduced using LASSO, and the optimal radiomics features with non-zero coefficients were selected through 10-fold cross-validation, ultimately extracting 13 radiomics features.

Establishment and validation of machine learning models

The selected radiomics features were modeled using Logistic regression and Random Forest (RF) machine learning algorithms with IPMS software, and divided into training and validation sets in a 7:3 ratio. The training set included 107 cases (77 GIST, 30 non-GIST), and the validation set included 46 cases (30 GIST, 16 non-GIST). The diagnostic performance of the two models in the training and validation sets was tested using receiver operating characteristic (ROC) curves, and the area under the curve (AUC) was compared using the Delong test. Decision curves were used to evaluate the net benefit of the two models.

Statistical analysis

SPSS 24.0 software was used for statistical analysis of clinical data. For measurement data, the Kolmogorov-Smirnov test was used to check for normal distribution. Normally distributed data were compared using the independent samples t-test and expressed as; $\bar{x} \pm s$ non-normally distributed data were compared using the Mann-Whitney test and expressed as median. Chi-square tests were used for comparing categorical data between groups. Modeling and comparison of the two models based on selected features were performed using IPMS software, with $P<0.05$ indicating statistically significant differences.

Results

The enhancement degree of GIST and non-GIST in the training set and the differences in age, maximum diameter, and tumor location distribution in the training and validation sets were statistically significant ($P<0.05$).

Table 1. *Comparison of basic data between GIST and non-GIST patients.*

Item	Training Set (n=107)		t/x²/Z	P	Validation Set (n=46)		t/x²/Z	P
	GIST (n=77)	Non-GIST (n=30)			GIST (n=30)	Non-GIST (n=16)		
Gender	-	-	0.084	0.771	-	-	0.646	0.421
Male	31 (40.26)	13 (43.33)	-	-	11 (36.67)	4 (25.00)	-	-
Female	46 (59.74)	17 (56.67)	-	-	19 (63.33)	12 (75.00)	-	-
Age (years)	61.2±1.4	53.6±2.1	21.747	<0.001	63.4±2.2	54.3±3.6	10.657	<0.001
Tumor Location	-	-	13.553	<0.001	-	-	16.893	<0.001
Stomach	65 (84.41)	15 (50.00)	-	-	28 (93.33)	5 (31.25)	-	-
Intestine	10 (12.99)	5 (16.67)	-	-	2 (6.67)	1 (6.25)	-	-
Abdominal cavity	2 (2.60)	1 (3.33)	-	-	0 (0.00)	1 (6.25)	-	-
Retroperitoneum	0 (0.00)	8 (26.67)	-	-	0 (0.00)	2 (12.50)	-	-
Pelvis	0 (0.00)	1 (3.33)	-	-	0 (0.00)	7 (43.75)	-	-

(Continued)

Maximum Diameter (mm)	34.2±5.7	42.3±4.9	6.854	＜0.001	38.5±4.6	52.1±9.2	6.715	＜0.001
Enhancement Pattern	-	-	0.229	0.631	-	-	1.932	0.164
Homogeneous	45 (58.44)	16 (53.33)	-	-	11 (36.67)	2 (12.50)	-	-
Heterogeneous	32 (41.56)	14 (46.67)	-	-	19 (63.33)	14 (87.50)	-	-
Calcification	14 (18.18)	3 (10.00)	0.555	0.455	6 (20.00)	2 (12.50)	0.053	0.817
Hemorrhage	2 (2.60)	4 (13.33)	2.891	0.089	0 (0.00)	1 (16.25)	-	1
Enhancement Degree	-	-	4.617	0.031	-	-	1.023	0.311
Mild	10 (12.99)	12 (40.00)	-	-	6 (20.00)	3 (18.75)	-	-
Moderate	21 (27.27)	7 (23.33)	-	-	10 (33.33)	8 (50.00)	-	-
Marked	46 (59.74)	11 (36.67)	-	-	14 (46.67)	5 (31.25)	-	-
Surface Ulceration	7 (9.09)	2 (6.67)	0.000	0.986	1 (3.33)	0 (0.00)	0.000	1.000
Lymphadenopathy	4 (5.19)	1 (3.33)	0.010	0.920	0 (0.00)	0 (0.00)	0.000	1.000

3.2 Radiomics Feature Selection Results

A total of 180 radiomics features were extracted using A.K software. Dimensionality reduction was performed on the high-dimensional data using LASSO regression, resulting in 13 radiomics features. These features are MaxIntensity, Percentile85, RelativeDeviation, Cluster-Prominence_AllDirection_offset1_SD, ClusterShade_angle45_offset1, GLCMEntropy_angle90_offset1, LongRunEmphasis_angle0_offset1, LongRunEmphasis_angle135_offset1, LongRunEmphasis_angle45_offset1, Long RunHighGreyLevelEmphasis_angle0_offset1, LongRunLowGreyLevelEmphasis_AllDirection_offset1, Maximum3DDiameter, and SurfaceVolumeRatio.

Radiomics prediction models

Based on the selected 13 radiomics features, Logistic regression and Random Forest (RF) models were established. The AUC of the Logistic regression model for distinguishing GIST from non-GIST in the training set was 0.753, and 0.582 in the validation set (Figure 1). The AUC of the RF model was 0.941 in the training set and 0.746 in the validation set (Figure 2). Comparison between the two groups showed that the diagnostic performance of the RF model was higher than that of the Logistic regression model ($P<0.05$) (Figure 3). Decision curve analysis showed that the net benefit of the RF model for distinguishing GIST was higher than considering all patients as GIST or non-GIST, and also higher than the Logistic regression model (Figure 4).

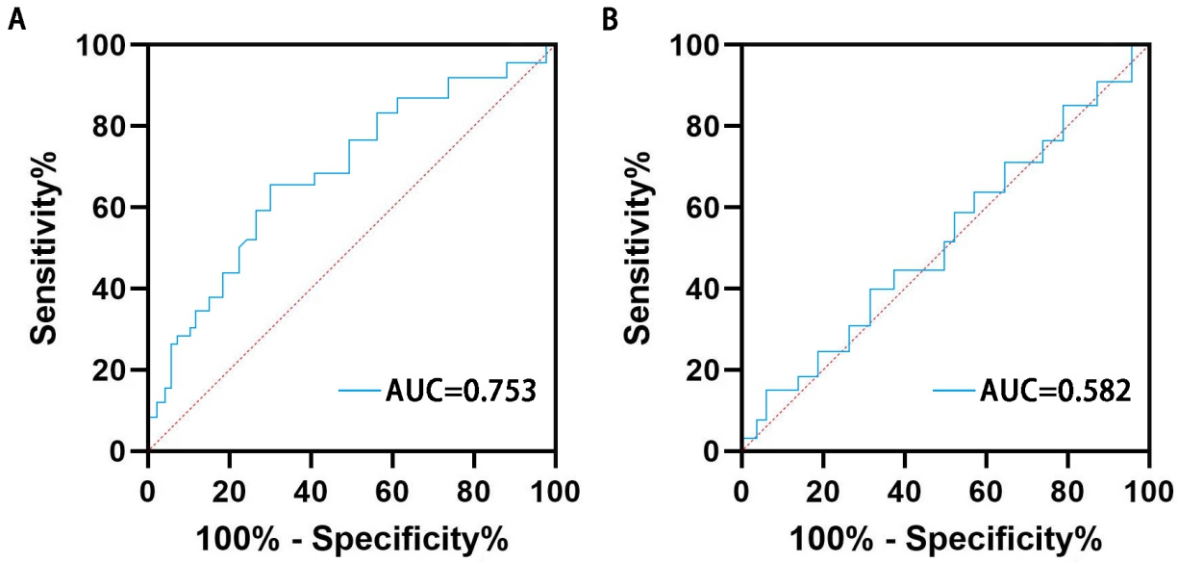

Figure 1. ROC curve of logistic regression model for distinguishing GIST from non-GIST. Note: A (Training Set); B (Validation Set).

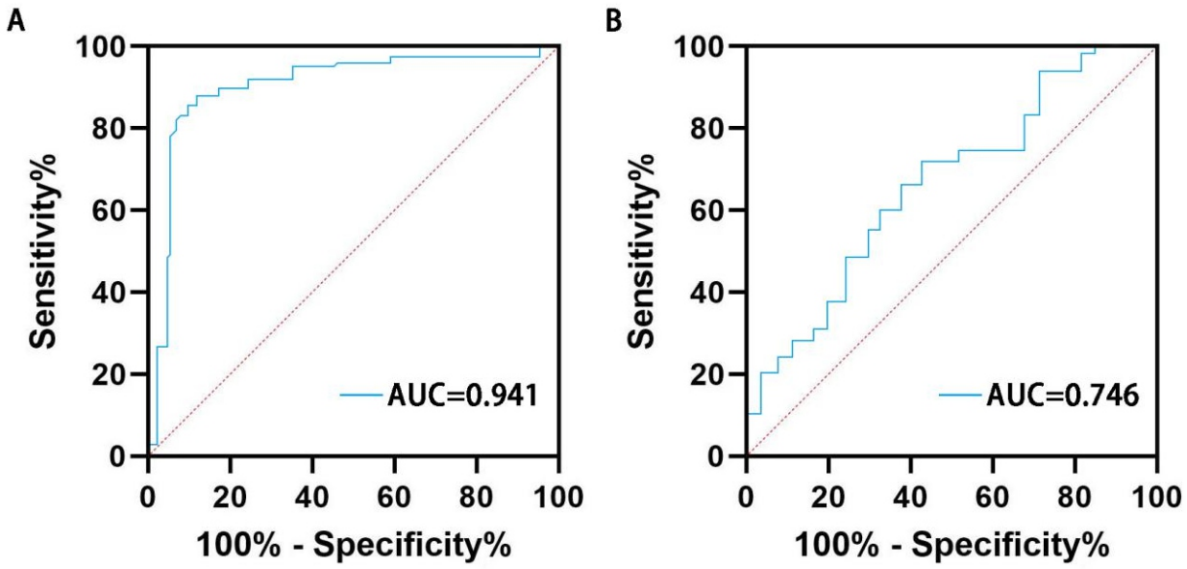

Figure 2. ROC Curve of RF model for distinguishing GIST from non-GIST. Note: A (Training Set); B (Validation Set).

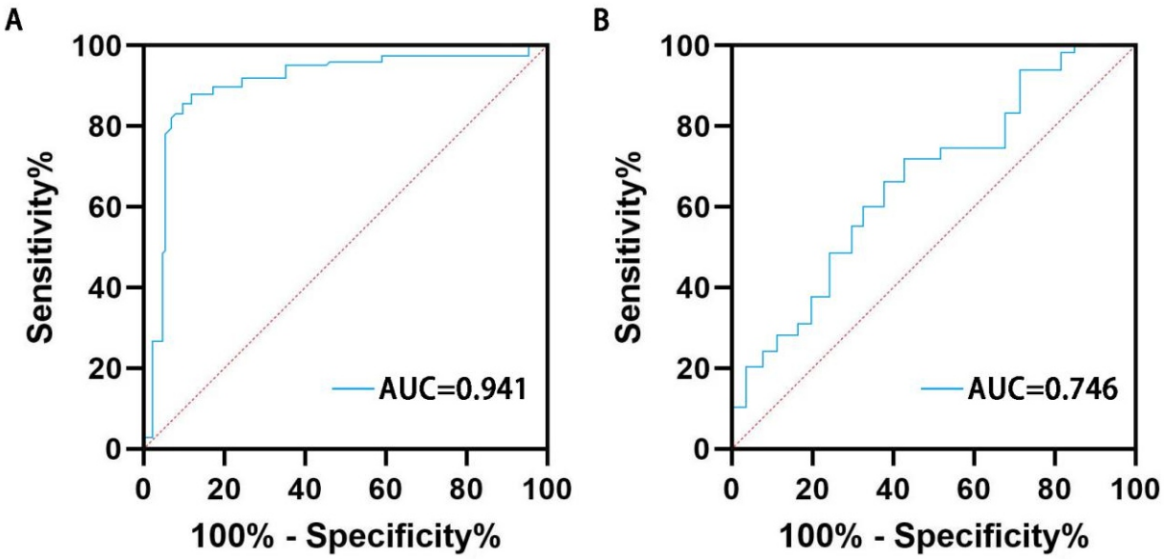

Figure 3. ROC curve comparison between logistic regression model and RF model for distinguishing GIST from non-GIST. Note: RF represents the RF model; Log represents the Logistic regression model.

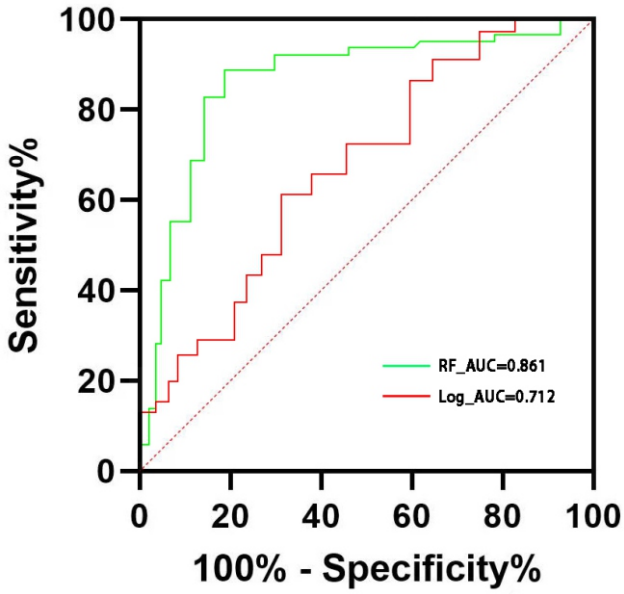

Figure 4. Decision curves of logistic regression model and RF model. Note: All represents all patients as GIST; None represents all patients as non-GIST.

Discussion

Comparison of basic data between GIST and non-GIST patients

In this study, the basic data of GIST and non-GIST patients showed significant differences in several aspects, specifically analyzed as follows: 1) Age difference: This study found that the average age of onset for GIST was older than that for non-GIST ($P<0.05$), consistent with previous studies [10]. Past research [11] indicated that the median age of onset for GIST is around 60 years, whereas the age of onset for leiomyomas and neurogenic tumors is generally lower. This may be due to the pathological characteristics and biological behavior of GIST, making it more common in older populations. 2) Tumor size difference: In this study, the tumor size difference between GIST and non-GIST patients was statistically significant ($P<0.05$), similar to the findings of Brinch et al. (2022) [12], indicating that GIST tumors are generally larger. However, another study [13] stated that the mean diameter of GIST, leiomyomas, and neurogenic tumors is similar with no statistical significance ($P>0.05$). The difference in these results may be related to the different proportions of non-GIST in the research samples. Additionally, GIST typically shows rapid growth and strong invasiveness, which may explain its larger tumor volume [14]. 3) Tumor location difference: This study found that the tumor location distribution between GIST and non-GIST patients was statistically significant ($P<0.05$). Among

mesenchymal tumors of the gastrointestinal tract, GIST predominantly occurs in the stomach (65/77), followed by the intestine (10/77), while non-GIST predominantly occurs in the stomach (15/30), followed by the retroperitoneum (8/30). This indicates that the tumor location can be an important basis for distinguishing GIST from non-GIST. The high incidence of GIST in the stomach is closely related to its pathological characteristics and the origin cells [15], while the higher incidence of non-GIST in the retroperitoneal area reflects the different tissue origins and growth characteristics of these tumors [16]. 4) Tumor enhancement feature difference: This study showed that the tumor enhancement features of GIST and non-GIST patients were significantly different ($P<0.05$). GIST tumors in patients mainly showed marked enhancement (46/77), while non-GIST tumors primarily showed mild enhancement (12/30). This difference may reflect the higher blood supply level and more active biological behavior of GIST. Previous studies [17] have also indicated that GIST typically has rich blood supply, showing significant imaging enhancement characteristics, while neurofibromas and other non-GIST tumors show more homogeneous tumors with lower enhancement levels. This difference can be used in imaging diagnosis to help differentiate GIST from other mesenchymal tumors.

Overall, this study, through detailed analysis of the basic data of GIST and non-GIST patients, confirmed the importance of multiple imaging features in differential diagnosis. These findings not only provide new auxiliary tools for clinical practice but also offer important references for future related research.

Diagnostic performance of radiomics in differentiating GIST from non-GIST

Radiomics technology, by high-throughput extraction of tumor internal features, has shown great potential in the diagnosis, treatment, and prognostic assessment of tumors [18]. Although radiomics has been applied in GIST research, it has mainly focused on risk stratification and genetic mutation status of GIST [19, 20], with relatively few studies on distinguishing between imaging-similar GIST, neurofibromas, and leiomyomas. Existing studies primarily analyze CT imaging features. For example, Choi et al. (2014) [21] used CT imaging features to differentiate GIST larger than 5cm from other mesenchymal tumors, but these features mainly rely on subjective analysis by radiologists, with significant inter-observer variability and a lack of objectivity. This study used radiomics methods, employing RF models and Logistic regression models to differentiate GIST from non-GIST. The results showed that the RF model exhibited high diagnostic performance in both the training set and validation set (training set AUC=0.941, validation set AUC=0.746), while the Logistic regression model had decent diagnostic performance in the training set (AUC=0.753), but poorer performance in the validation set (AUC=0.582). This difference indicates that the RF model has better stability and adaptability in handling high-dimensional radiomics features and complex data disturbances. Decision curve analysis further showed that when the probability threshold was 20% to 90%, the net benefit of the RF model in distinguishing GIST was significantly higher than considering all patients as GIST or non-GIST and also higher than the Logistic regression model. This means that the RF model not only has higher discriminatory power statistically but also has greater practical value in clinical applications.

Existing literature also supports the superiority of the RF model in radiomics applications. For instance, Parmar et al. (2015) [22] and others used 12 machine learning models to predict the overall survival rate of lung cancer, showing that the RF-based machine learning model achieved the highest predictive performance (AUC=0.66±0.03). Additionally, Wang et al. (2020) [23] in their MRI radiomics study, using four feature selection methods and three machine learning models to differentiate the malignancy of soft tissue masses, found that LASSO regression feature selection combined with the RF model showed the highest AUC in two validation cohorts (0.86 and 0.82, respectively). These results are consistent with those of this study, further validating the effectiveness and stability of the RF model in radiomics analysis. As a powerful and flexible machine learning algorithm, RF can handle high-dimensional data and complex feature interactions, making it particularly suitable for feature selection and analysis in radiomics. Its stability in handling data disturbances makes it an ideal choice for radiomics-based predictive research.

In summary, this study successfully established an efficient model for differentiating GIST from non-GIST using radiomics technology and machine learning algorithms. The RF model performed excellently in handling high-dimensional imaging data and complex features, significantly outperforming the traditional Logistic regression model. This not only provides a new and effective auxiliary diagnostic tool for clinical practice but also offers important references for future applications of radiomics in tumor differential diagnosis. Future research should further validate the stability and generalizability of the RF model in larger sample sizes and multi-center data to promote the wide application of radiomics technology in clinical diagnosis.

In conclusion, the machine learning model based on radiomics features has good diagnostic value in predicting GIST and other mesenchymal tumor pathological subtypes, with the RF model showing superior diagnostic value compared to the Logistic regression model. However, it is also necessary to note some shortcomings in this study that need improvement, such as: 1) Small sample size: The sample size of this study is relatively small, which may affect the credibility and applicability of the results and limit the statistical significance of some results. 2) Retrospective analysis: This study used retrospective analysis, which may have information bias and treatment selection bias. 3) Single-center study: This study was conducted in only one hospital, which may limit the external applicability of the research results. 4) Manual segmentation errors: All ROI in this study were manually delineated, inevitably introducing some potential human errors. Therefore, in future research, we will enhance the study design and results by increasing the sample size and improving the study design to further enhance the scientific and practical aspects of the research.

Bibliography

1) Sharma AK, Kim TS, Bauer S, Sicklick JK. Gastrointestinal Stromal Tumor:

New Insights for a Multimodal Approach. *Surg Oncol Clin N Am* 2022;
2. Schaefer IM, DeMatteo RP, Serrano C. The GIST of Advances in Treatment of Advanced Gastrointestinal Stromal Tumor. *Am Soc Clin Oncol Educ Book* 2022; 42: 1-15.
3. Serrano C, George S. Gastrointestinal Stromal Tumor: Challenges and Opportunities for a New Decade. *Clin Cancer Res* 2020; 26(19): 5078-85.
4. Tsai MK, Chen HY, Chuang ML et al. Gastric Calcifying Fibrous Tumor: An Easy Misdiagnosis as Gastrointestinal Stromal Tumor-A Systemic Review. *Medicina (Kaunas)* 2020; 56(10): 541.
5. Miranda J, Horvat N, Araujo-Filho JAB et al. The Role of Radiomics in Rectal Cancer. *J Gastrointest Cancer* 2023; 54(4): 1158-80.
6. Russo L, Charles-Davies D, Bottazzi S et al. Radiomics for clinical decision support in radiation oncology. *Clin Oncol (R Coll Radiol)* 2024; 36(8): e269-e281.
7. Kummar S, Lu R. Using Radiomics in Cancer Management. *JCO Precis Oncol* 2024; 8: e2400155.
8. Horvat N, Papanikolaou N, Koh DM. Radiomics Beyond the Hype: A Critical Evaluation Toward Oncologic Clinical Use. *Radiol Artif Intell* 2024; 6(4): e230437.
9. Mantese G. Gastrointestinal stromal tumor: epidemiology, diagnosis, and treatment. *Curr Opin Gastroenterol* 2019; 35(6): 555-9.
10. Mechahougui H, Michael M, Friedlaender A. Precision Oncology in Gastrointestinal Stromal Tumors. *Curr Oncol* 2023; 30(5): 4648-62.
11. Dudzisz-Śledź M, Bylina E, Teterycz P, Rutkowski P. Treatment of Metastatic Gastrointestinal Stromal Tumors (GIST): A Focus on Older Patients. *Drugs Aging* 2021; 38(5): 375-96.
12. Brinch CM, Aggerholm-Pedersen N, Hogdall E, Krarup-Hansen A. Medical oncological treatment for patients with Gastrointestinal Stromal Tumor (GIST) - A systematic review. *Crit Rev Oncol Hematol* 2022; 172: 103650.
13. Apte SS, Radonjic A, Wong B et al. Preoperative imaging of gastric GISTs underestimates pathologic tumor size: A retrospective, single institution analysis. *J Surg Oncol* 2021; 124(1): 49-58.
14. Ahmed M. Recent advances in the management of gastrointestinal stromal tumor. *World J Clin Cases* 2020; 8(15): 3142-55.
15. Paganini AM, Quaresima S, Balla A et al. Clinicopathological Features and Surgical Management of Gastrointestinal Stromal Tumors: State-of-the-Art. In: Morgado-Diaz JA, ed. *Gastrointestinal Cancers*. Brisbane (AU): Exon Publications; September 30, 2022.
16. Davila RE. A Gastroenterologist's Approach to the Diagnosis and Management of Gastrointestinal Stromal Tumors. *Gastroenterol Clin North Am* 2022; 51(3): 609-24.
17. Arzoun H, Srinivasan M, Adam M et al. Evaluation of and Current Trends in the Management of Gastrointestinal Stromal Tumors: A Systematic Review. *Cureus* 2022; 14(7): e26848.
18. Bo Z, Song J, He Q et al. Application of artificial intelligence radiomics in the diagnosis, treatment, and prognosis of hepatocellular carcinoma. *Comput Biol Med* 2024; 173: 108337.
19. Zhuo M, Guo J, Tang Y et al. Ultrasound radiomics model-based nomogram for predicting the risk Stratification of gastrointestinal stromal tumors. *Front Oncol* 2022; 12: 905036.
20. Cappello G, Giannini V, Cannella R et al. A mutation-based radiomics signature predicts response to imatinib in Gastrointestinal Stromal Tumors (GIST). *Eur J Radiol Open* 2023; 11: 100505.
21. Choi YR, Kim SH, Kim SA, et al. Differentiation of large (≥5cm) gastrointestinal stromal tumors from benign subepithelial tumors in the stomach: radiologists' performance using CT. *Eur J Radiol* 2014; 83(2): 250-60.
22. Parmar C, Grossmann P, Bussink J et al. Machine Learning methods for Quantitative Radiomic Biomarkers. *Sci Rep* 2015; 5: 13087.
23. Wang H, Zhang J, Bao S et al. Preoperative MRI-Based Radiomic Machine-Learning Nomogram May Accurately Distinguish Between Benign and Malignant Soft-Tissue Lesions: A Two-Center Study. *J Magn Reson Imaging* 2020; 52(3): 873-82.